PROBING THE MAGNETIC FIELD OF 3C 279

by Sebastian Kiehlmann
on behalf of the Quasar Movie Project team

Max Planck Institute for Radio Astronomy,
Auf dem Hügel 69, 53121 Bonn, Germany

The Quasar Movie Project

MAX-PLANCK-GESELLSCHAFT

IMPRS astronomy & astrophysics Bonn and Cologne

II. Polarization of 3C 279

degree of linear polarization:

- mean $\langle P \rangle = 12\ \%$
- variation $\sigma(P) = 8\ \%$

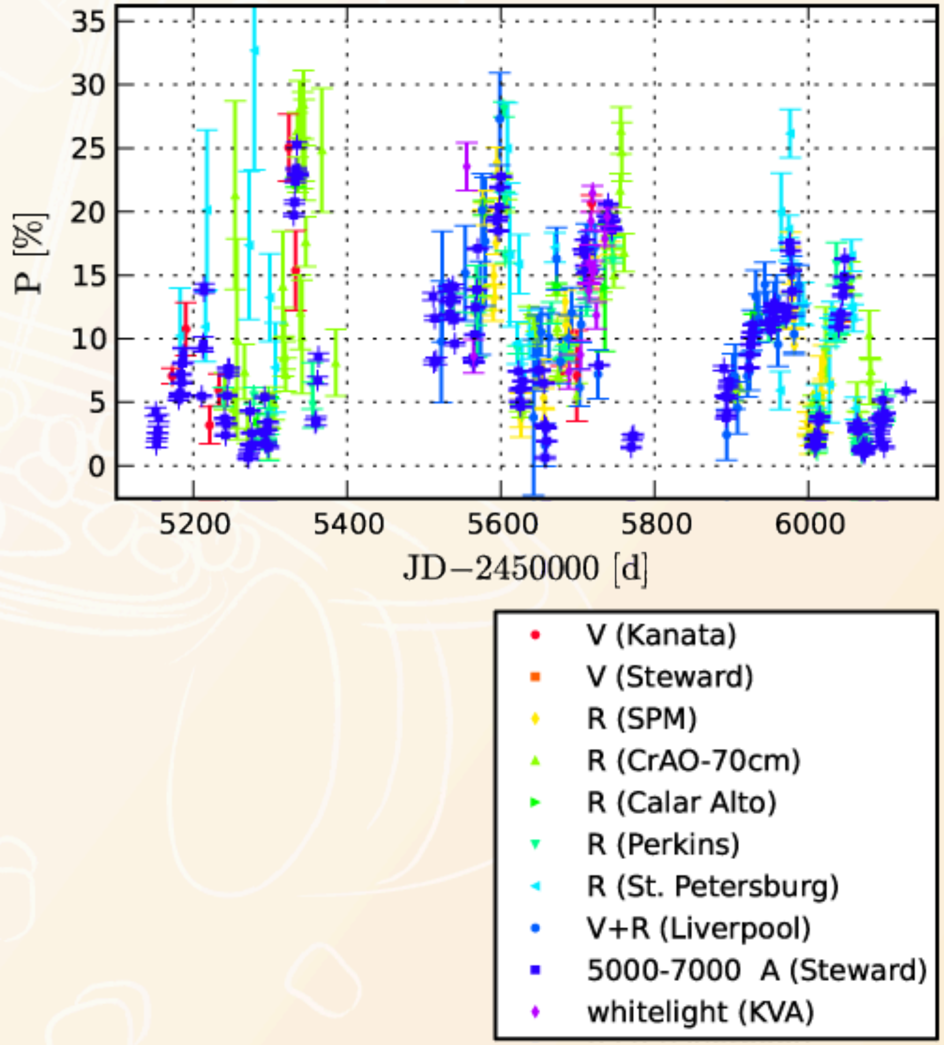

Fig. 1a: Optical, linear polarization degree of 3C 279

II. Polarization of 3C 279

degree of linear polarization

Optical electric vector position angle (EVPA)

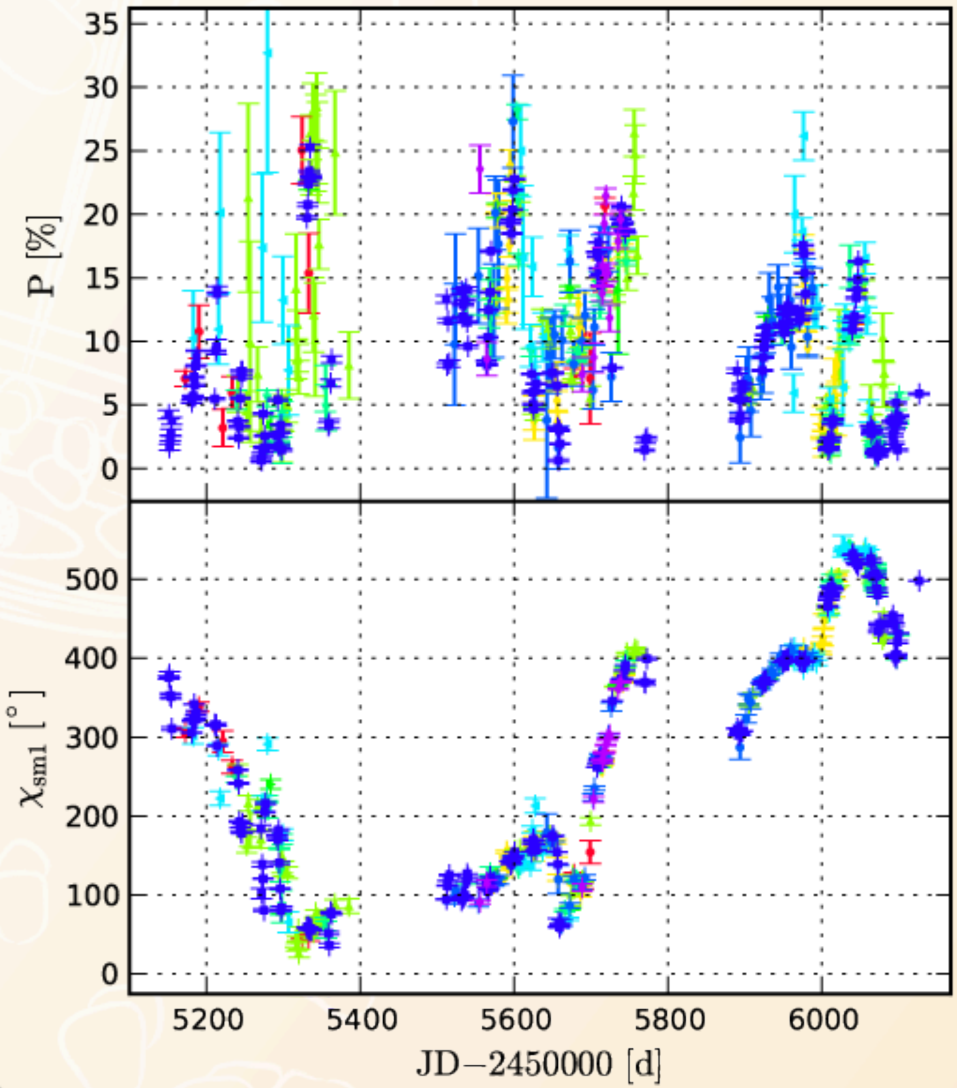

Fig. 1b: Optical, linear polarization degree and EVPA of 3C 279

II. Polarization of 3C 279

object	EVPA rotation	time interval	explanation	reference
OJ 287	120 °	7 d	Helical motion in a helical magnetic field	Kikuchi et al., 1988
BL Lac	240 °	5 d		Marscher et al., 2008
PKS 1510-089	720 °	50 d		Marscher et al., 2010
3C 279	↺ 300 °	60 d		Larionov et al., 2008
3C 279	↻ 208 °	12 d	Bent jet	Abdo et al., 2010

γ- ray flaring

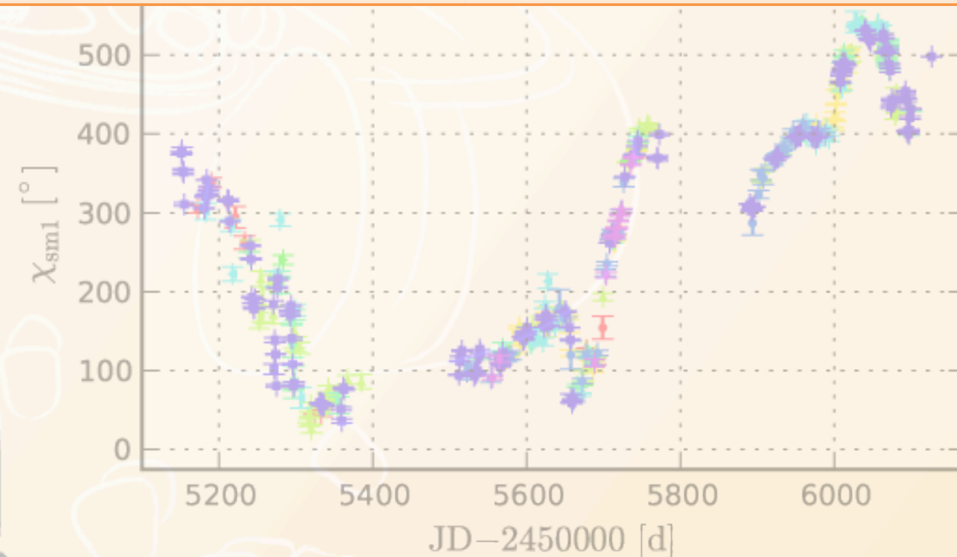

Fig. 1b: Optical, linear polarization degree and EVPA of 3C 279

III. The 180° ambiguity

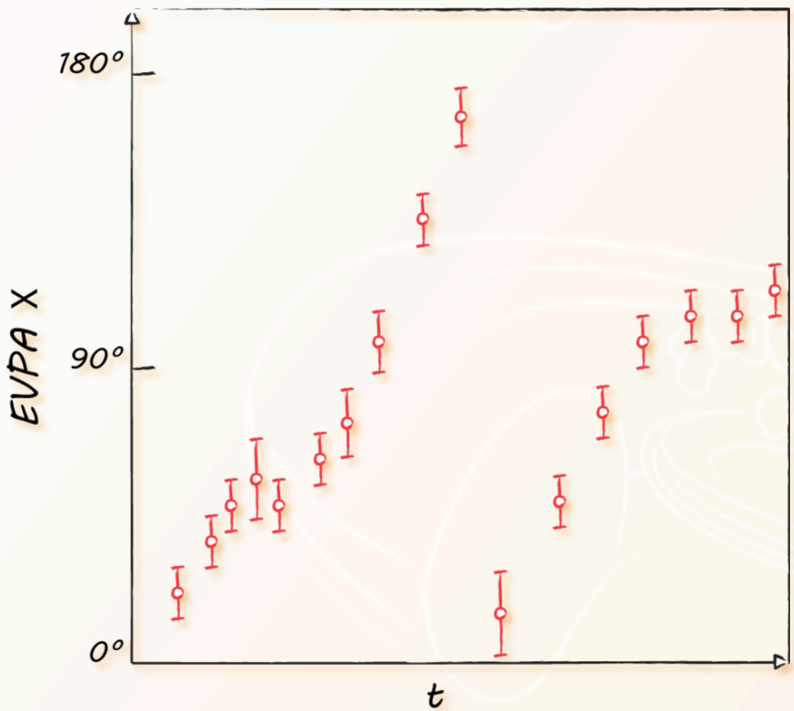

- **Assumption:** smooth variation
- **Question:**
  - Valid assumption?
  - Reliability?

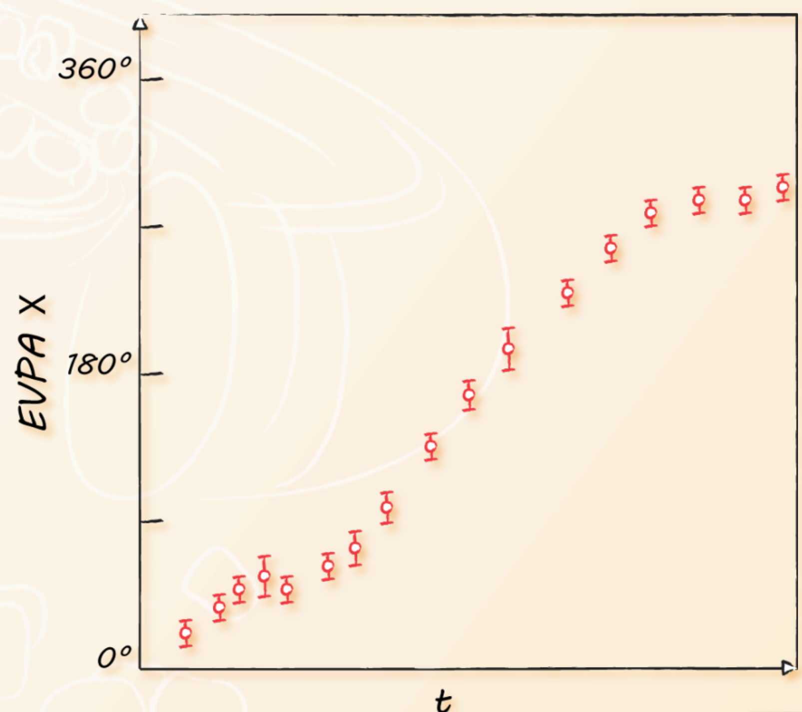

Fig. 2a: Sketched EVPA curve

Fig. 2b: Sketched modified EVPA curve

SEBASTIAN KIEHLMANN, DIPL.-PHYS.
MAX-PLANCK INSTITUT FÜR RADIOASTRONOMIE, BONN

III. The 180° ambiguity

III.a Smoothing methods

Method 1:

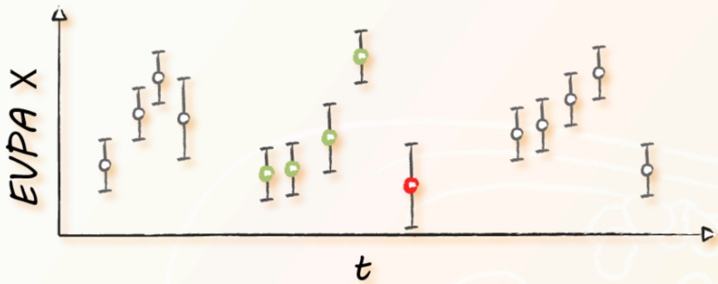

$$\chi_{ref,i} = \langle [\chi_{i-1-N}, \chi_{i-1}] \rangle$$

$$N = 4$$

if $|\chi_i - \chi_{ref,i}| > 90°$

$$\chi_{mod,i} = \chi_i \pm n \cdot 180°$$

Method 2:

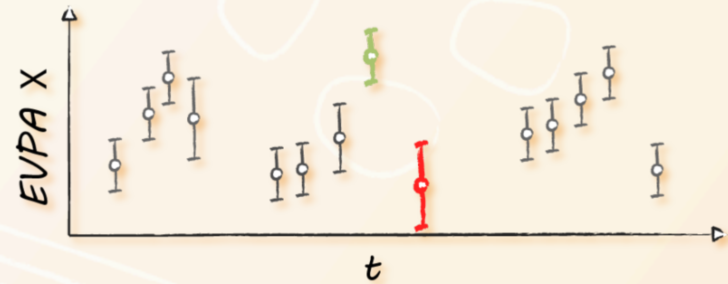

$$\Delta\chi_i = |\chi_i - \chi_{i-1}| - \sqrt{\sigma^2(\chi_i) + \sigma^2(\chi_{i-1})}$$

if $\Delta\chi_i > 90°$

Sebastian Kiehlmann, Dipl.-Phys.
Max-Planck Institut für Radioastronomie, Bonn

III. The 180° ambiguity

III.c Test 2: assumption of smoothness

Random walk model:

e.g. F. D'Arcangelo et al., ApJ 2007

Total cells $N = 54 \propto \langle P \rangle^{-2}$

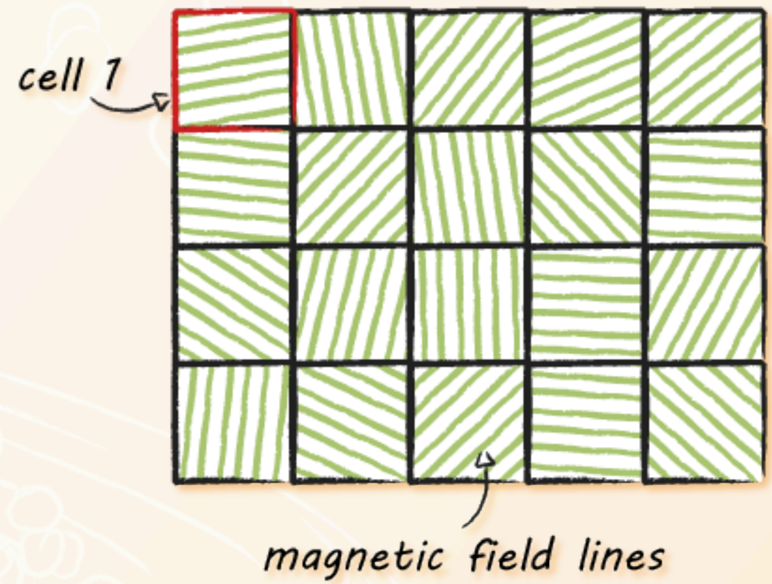

Fig. 4a: Sketched cells of the random walk process

III. The 180° ambiguity

III.c Test 2: assumption of smoothness

Random walk model:

e.g. F. D‘Arcangelo et al., ApJ 2007

Total cells $N = 54 \propto \langle P \rangle^{-2}$

Vary Cells $N_{var} = 35 \propto \sigma(P)/\langle P \rangle$

Mean time step: 3 d

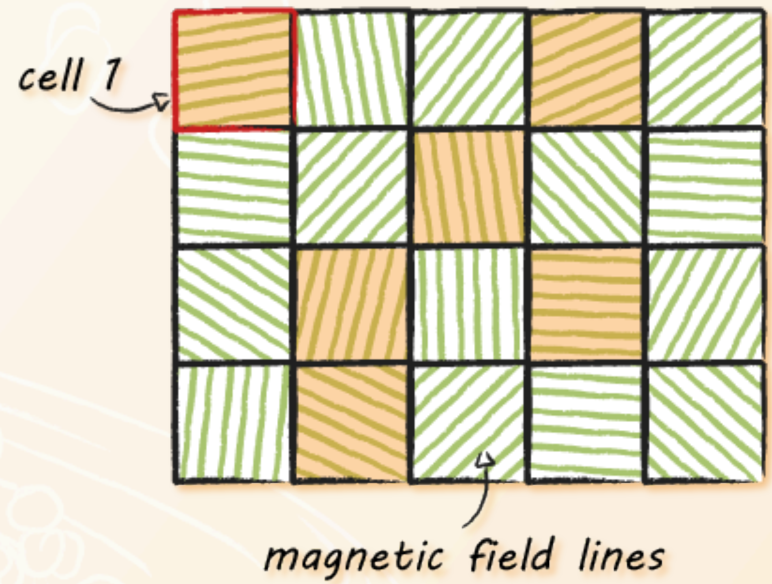

Fig. 4b: Sketched cells of the random walk process

III.c Test 2: assumption of smoothness

Random walk model:

e.g. F. D'Arcangelo et al., ApJ 2007

Total cells $N = 54 \propto \langle P \rangle^{-2}$

Vary Cells $N_{var} = 35 \propto \sigma(P)/\langle P \rangle$

Mean time step: 3 d

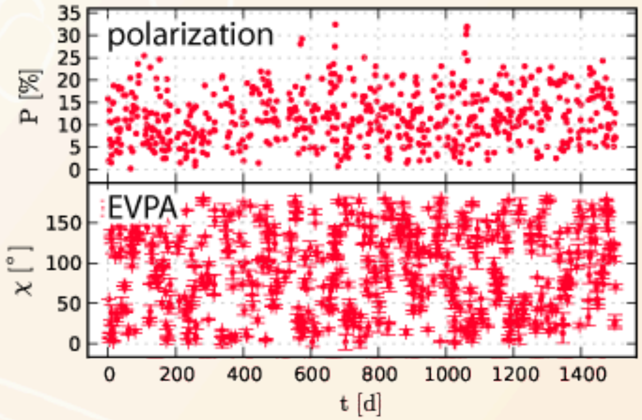

Fig. 5a: Random EVPA variation

III. The 180° ambiguity

III.c Test 2: assumption of smoothness

1,000,000 simulations

EVPA amplitude A_χ:	Method 1:	Method 2:
$A_\chi > 180°$:	> 99.5 %	> 98.5 %
$A_\chi > 360°$:	43 %	43 %

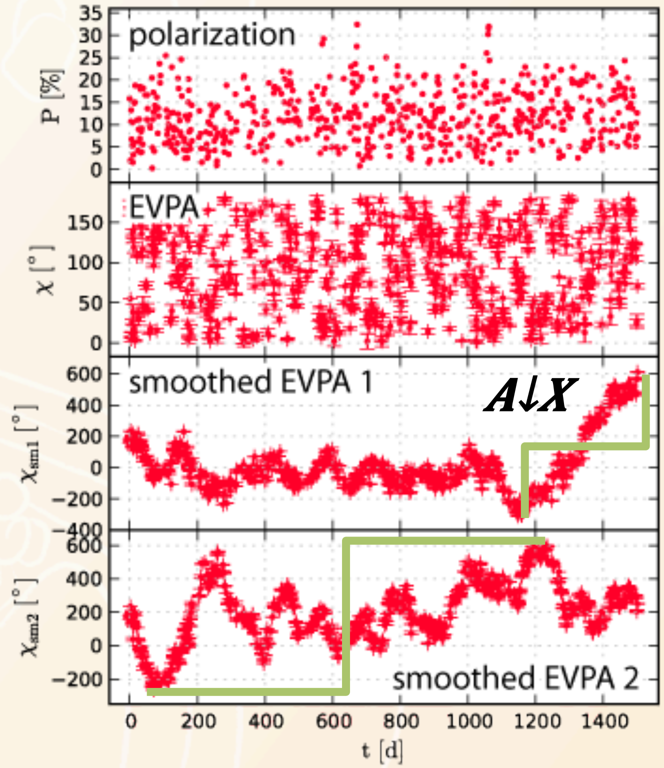

Fig. 5b: Random EVPA variation, smoothed

III. The 180° ambiguity

III.c Test 2: assumption of smoothness

1,000,000 simulations

EVPA amplitude A_χ:	Method 1:	Method 2:
$A_\chi > 180°$:	> 99.5 %	> 98.5 %
$A_\chi > 360°$:	43 %	43 %
$\chi_{sm1} = \chi_{sm2}$:		1 %

$$(\Delta\chi/\Delta t)_i = \frac{\chi_i - \chi_{i-1}}{t_i - t_{i-1}}$$

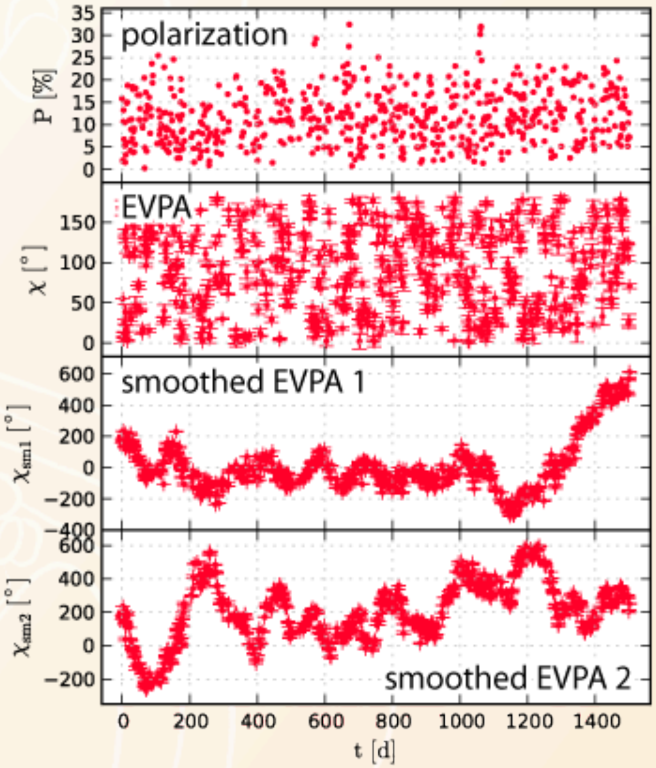

Fig. 5b: Random EVPA variation, smoothed

III. The 180° ambiguity

III.c Test 2: assumption of smoothness

1,000,000 simulations

EVPA amplitude A_χ:	Method 1:	Method 2:
$A_\chi > 180°$:	> 99.5 %	> 98.5 %
$A_\chi > 360°$:	43 %	43 %
$\chi_{sm1} = \chi_{sm2}$:		1 %

$$\left(\frac{\Delta \chi}{\Delta t}\right)_i = \frac{\chi_i - \chi_{i-1}}{t_i - t_{i-1}}$$

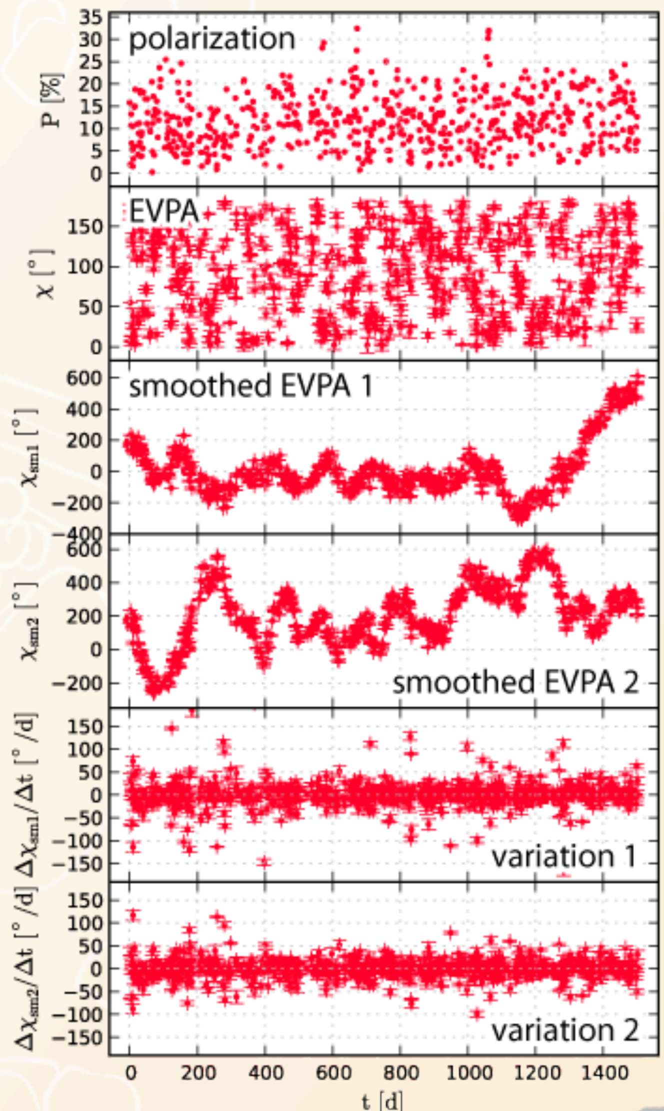

Fig. 5c: Random EVPA variation, smoothed, p-t-p variation

III. The 180° ambiguity

III.c Test 2: assumption of smoothness

1,000,000 simulations

EVPA amplitude A_χ:	Method 1:	Method 2:
$A_X > 180°$:	> 99.5 %	> 98.5 %
$A_X > 360°$:	43 %	43 %
$\chi_{sm1} = \chi_{sm2}$:		1 %

$$s = \langle |(\Delta X/\Delta t)_i - m| \rangle \quad with \quad m = \langle (\Delta X/\Delta t)_i \rangle$$

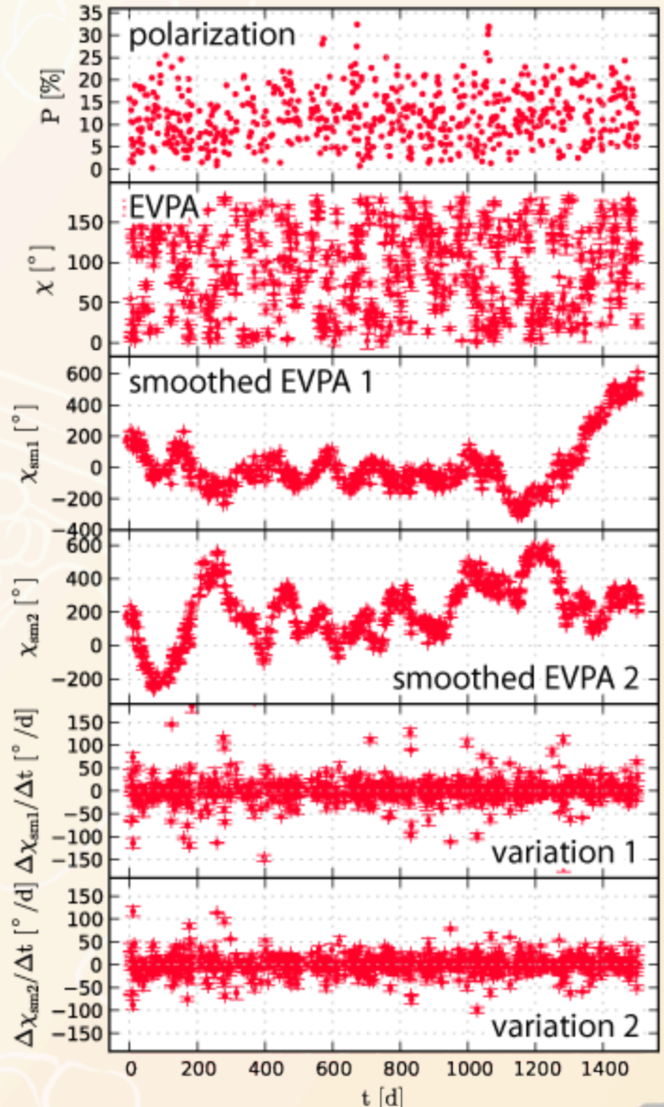

Fig. 5c: Random EVPA variation, smoothed, p-t-p variation

III. The 180° ambiguity

III.c Test 2: assumption of smoothness

1,000,000 simulations

EVPA amplitude A_{χ}:	Method 1:	Method 2:
$A_{\chi} > 180°$:	> 99.5 %	> 98.5 %
$A_{\chi} > 360°$:	43 %	43 %
Variation estimator *s*:		
$s < 6\,°/d$:	0 %	0 %
$s < 10\,°/d$:	0.1 %	0.3 %
$s < 20\,°/d$:	76 %	98 %
$\langle s \rangle =$	18 °/d	15 °/d
$\chi_{sm1} = \chi_{sm2}$:		1 %

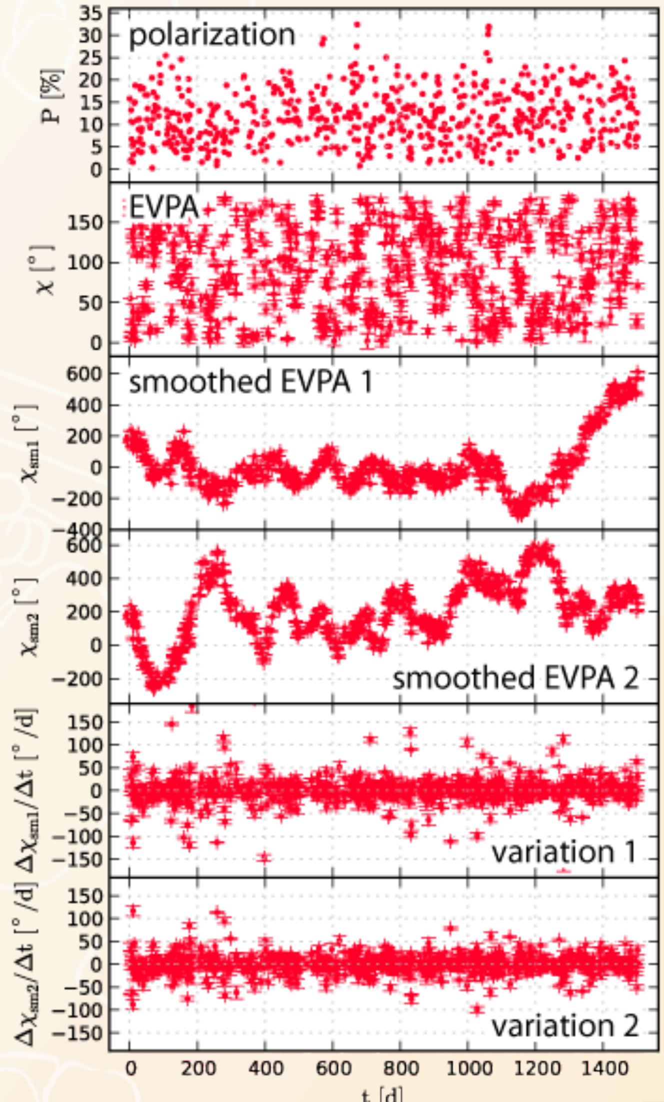

Fig. 5c: Random EVPA variation, smoothed, p-t-p variation

3C 279 observation (optical)

Random walk simulation

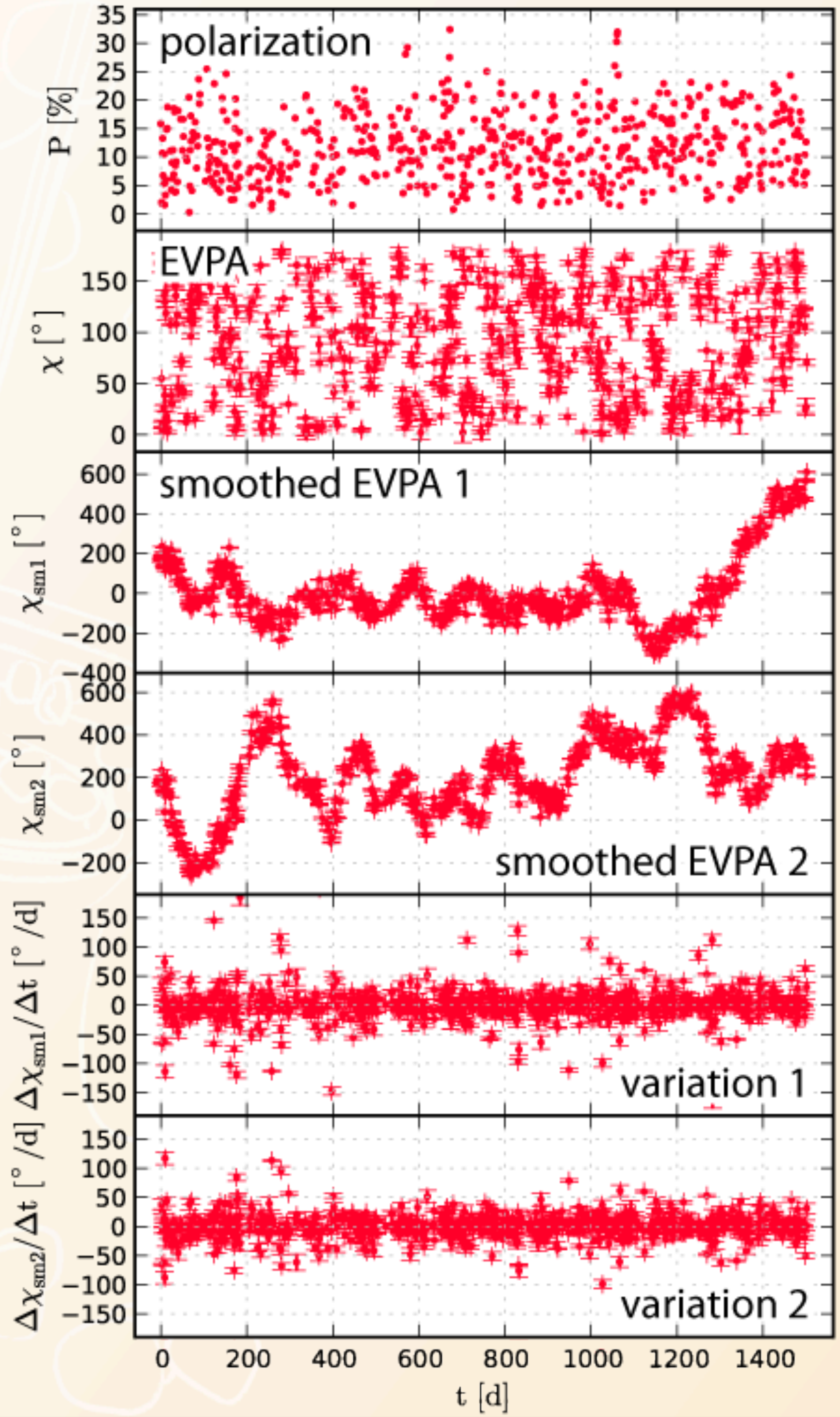

→ 3C 279 observation (optical) →

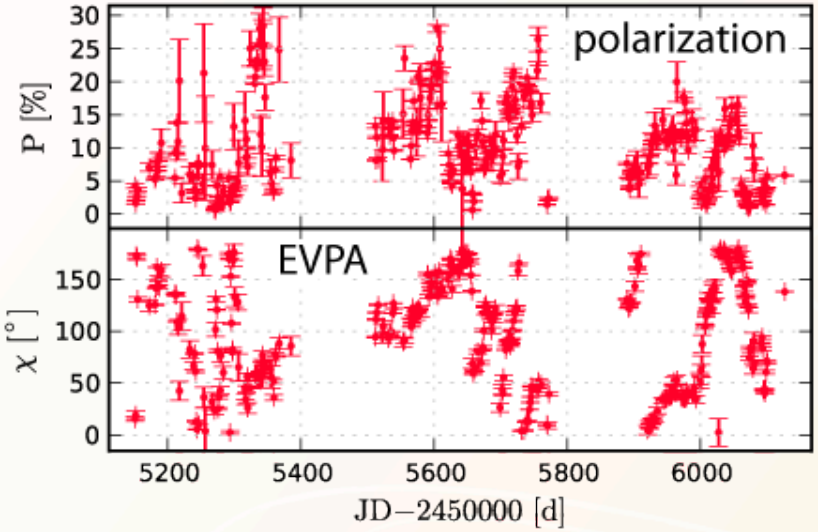

→ Random walk simulation →

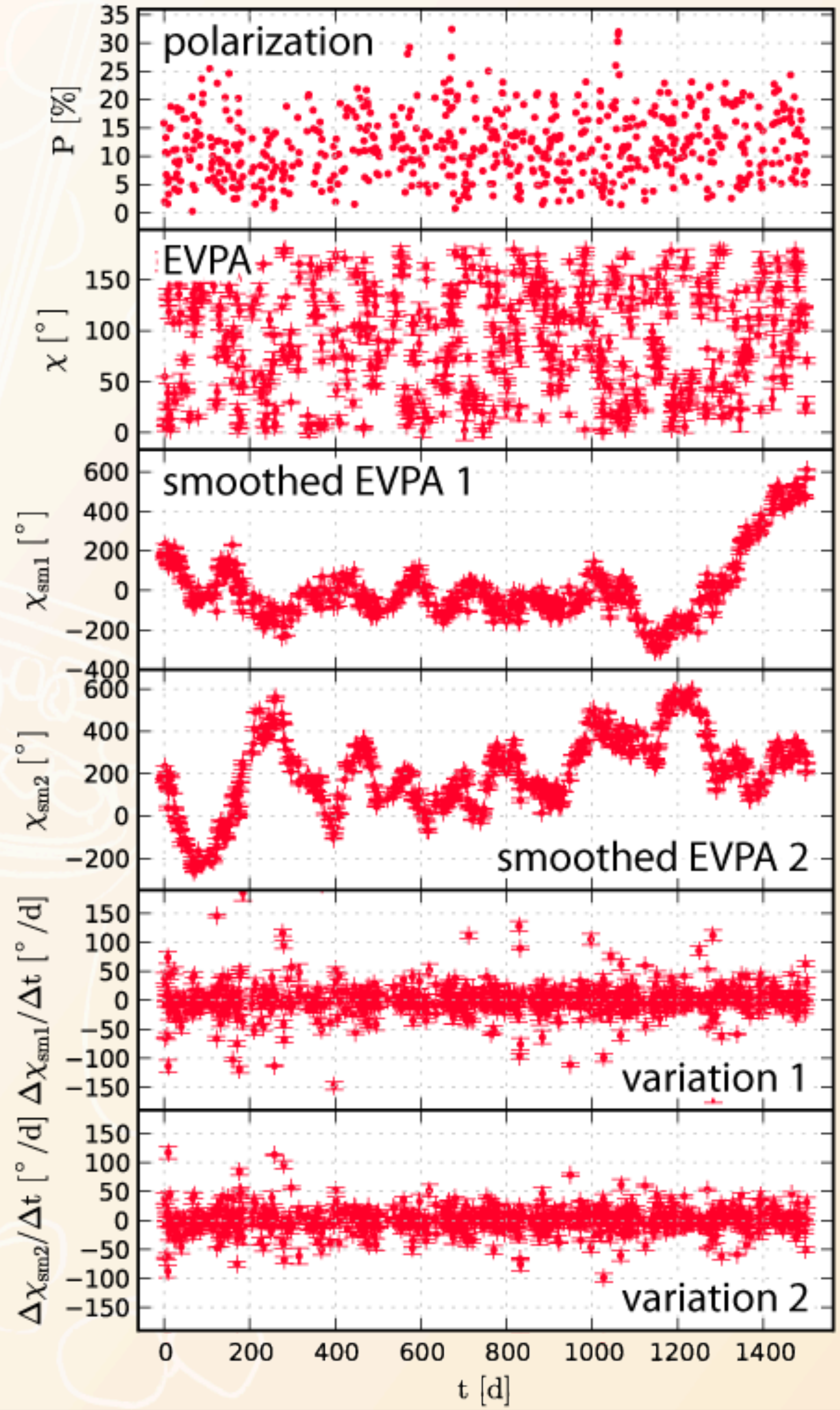

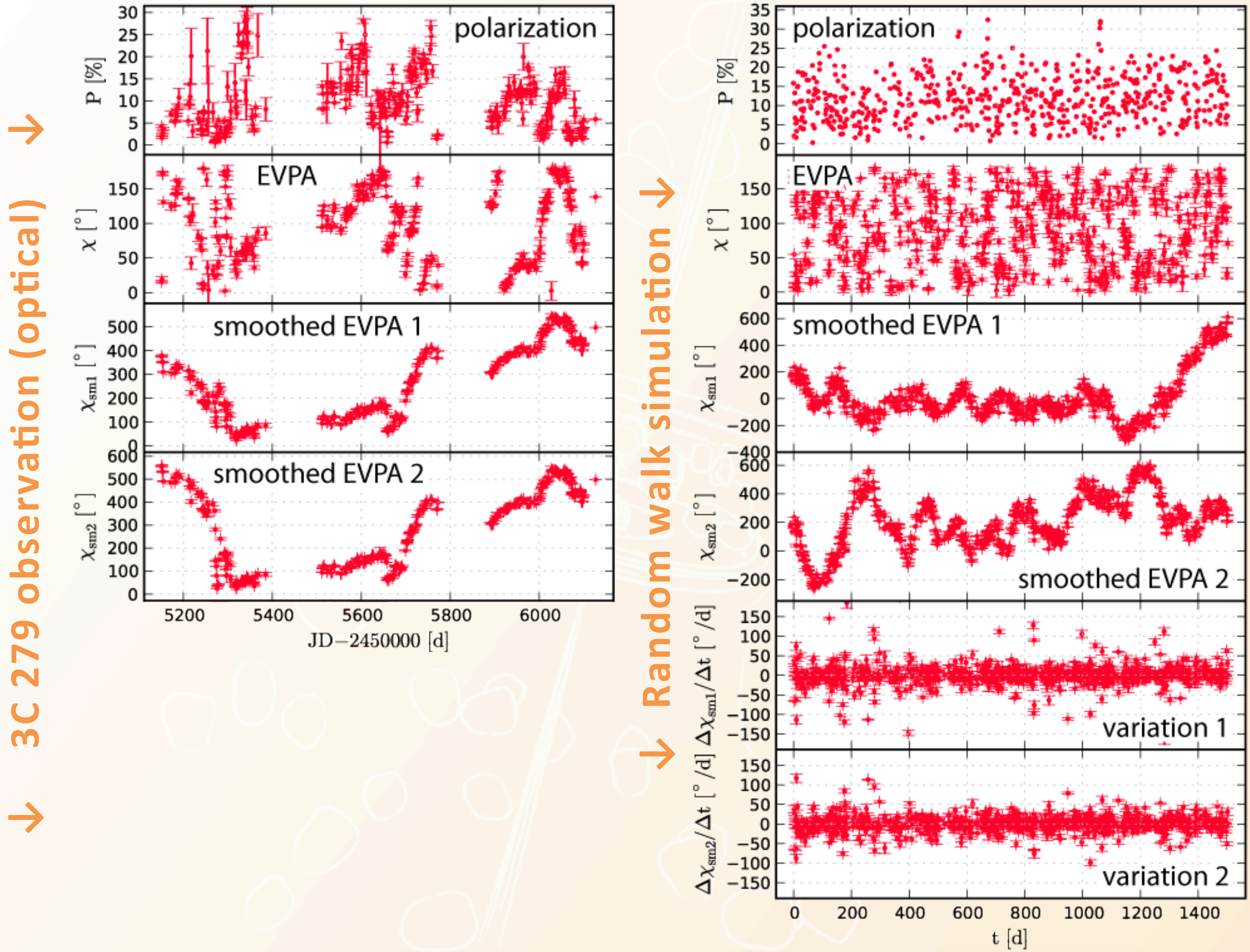

3C 279 observation (optical)
polarization
P [%]
EVPA
χ [°]
smoothed EVPA 1
χ_{sm1} [°]
smoothed EVPA 2
χ_{sm2} [°]
JD−2450000 [d]
Random walk simulation
polarization
P [%]
EVPA
χ [°]
smoothed EVPA 1
χ_{sm1} [°]
smoothed EVPA 2
χ_{sm2} [°]
variation 1
$\Delta\chi_{sm1}/\Delta t$ [°/d]
variation 2
$\Delta\chi_{sm2}/\Delta t$ [°/d]
t [d]

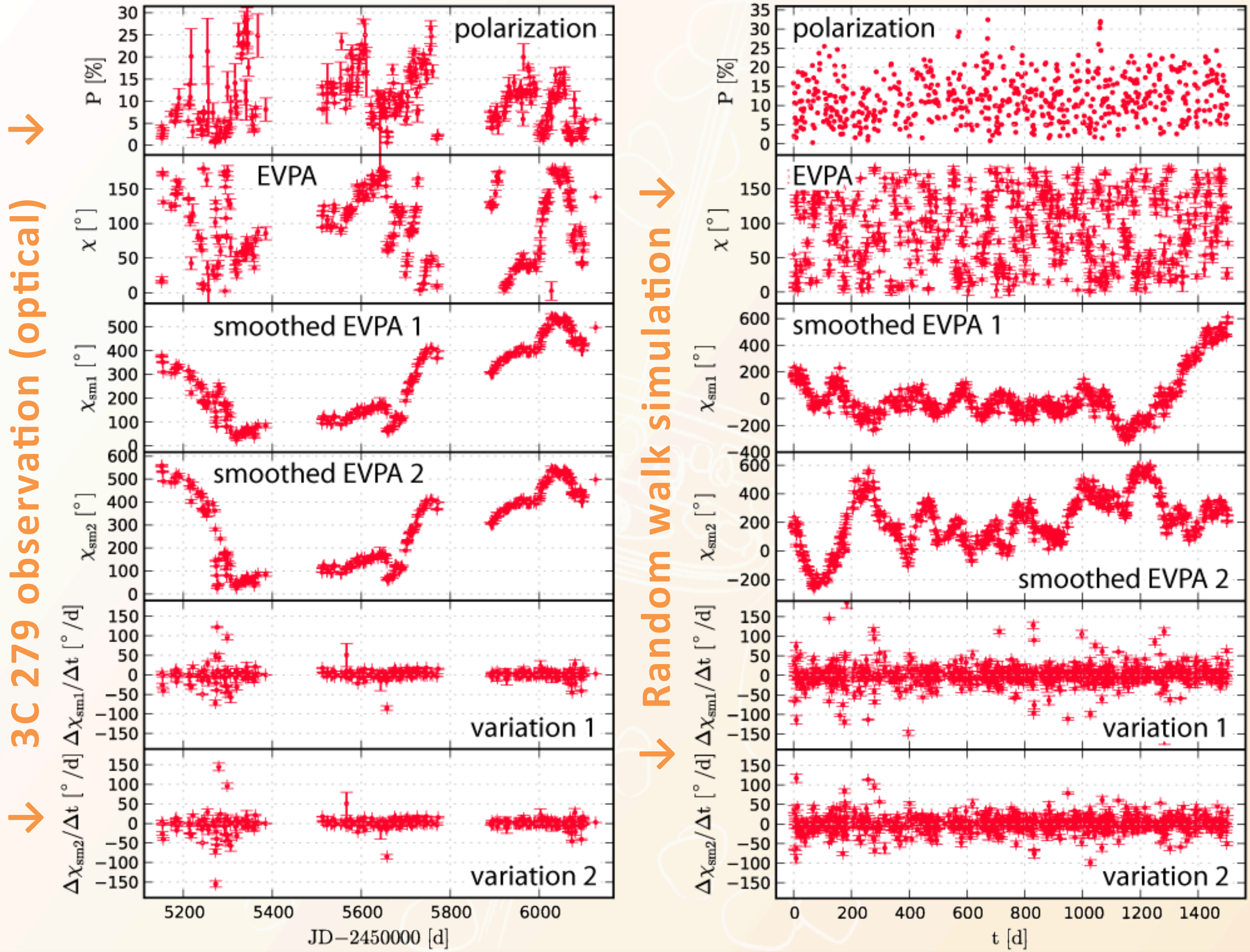

3C 279 observation (optical)
Random walk simulation
polarization
P [%]
EVPA
χ [°]
smoothed EVPA 1
χ_{sm1} [°]
smoothed EVPA 2
χ_{sm2} [°]
variation 1
$\Delta\chi_{sm1}/\Delta t$ [°/d]
variation 2
$\Delta\chi_{sm2}/\Delta t$ [°/d]
JD−2450000 [d]
5200 5400 5600 5800 6000
t [d]
0 200 400 600 800 1000 1200 1400

IV. Polarization of 3C 279

IV.a EVPA smoothness

Epoch	EVPA	s [°/d]	$\chi_{sm1} = \chi_{sm2}$
I	↓	32(5)	no

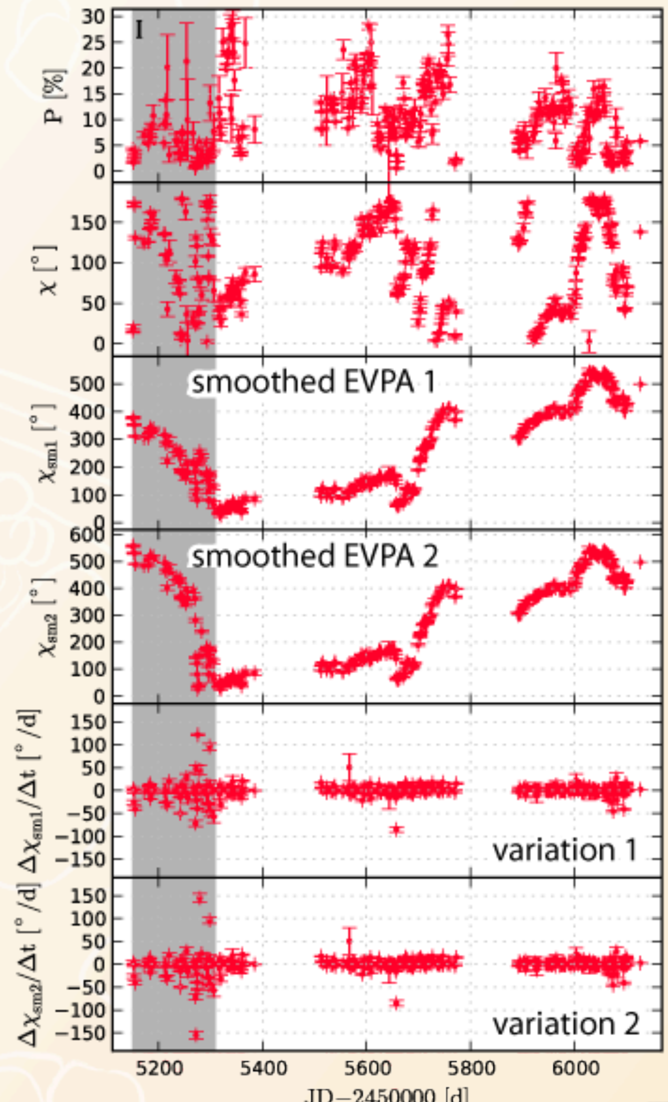

Fig. 6a: 3C 279 optical polarization

IV. Polarization of 3C 279

IV.a EVPA smoothness

Epoch	EVPA	s [°/d]	$\chi_{sm1} = \chi_{sm2}$
I	↓	32(5)	no
II	↑		

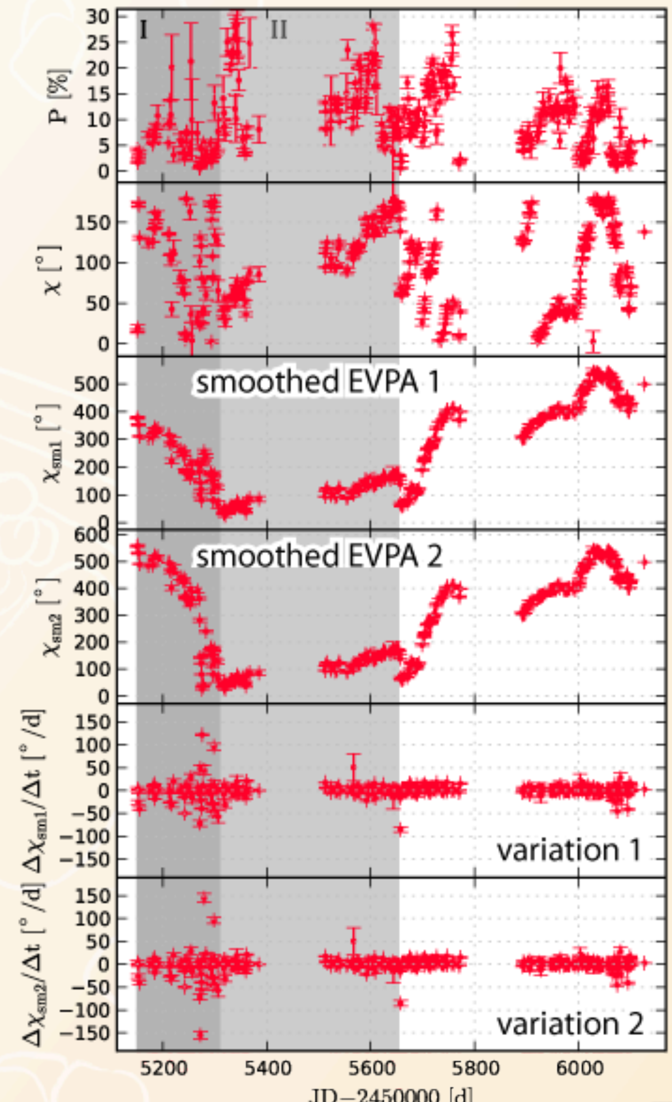

Fig. 6b: 3C 279 optical polarization

IV. Polarization of 3C 279

IV.a EVPA smoothness

Epoch	EVPA	s [°/d]	$\chi_{sm1} = \chi_{sm2}$
I	↓	32(5)	no
II	↑		
III	↓		

Fig. 6c: 3C 279 optical polarization

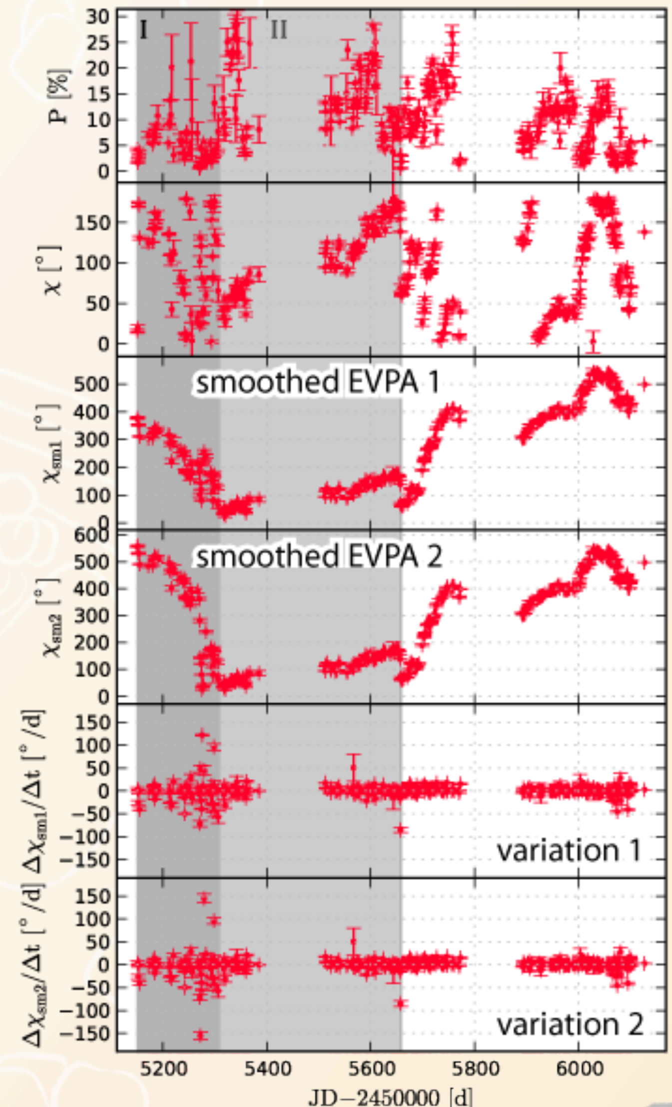

IV. Polarization of 3C 279

IV.a EVPA smoothness

Epoch	EVPA	s [°/d]	$\chi_{sm1} = \chi_{sm2}$
I	↓	32(5)	no
II	↑		
III	↓		
IV	↑		

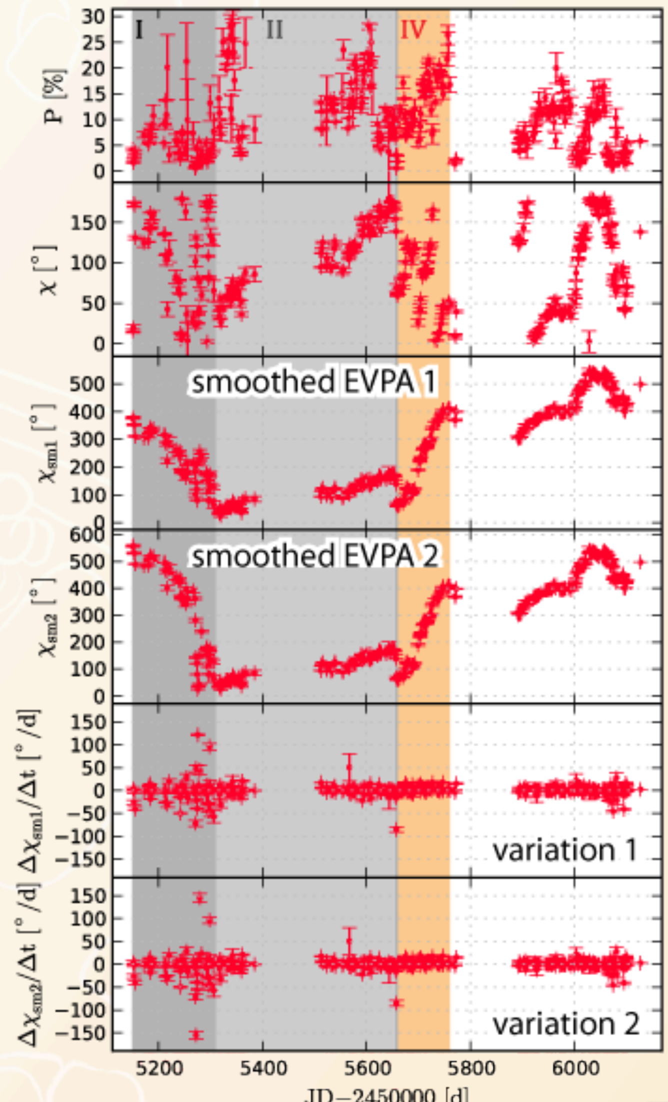

Fig. 6d: 3C 279 optical polarization

IV. Polarization of 3C 279

IV.a EVPA smoothness

Epoch	EVPA	s [°/d]	$\chi_{sm1} = \chi_{sm2}$
I	↓	32(5)	no
II	↑		
III	↓		
IV	↑		
V	↑		

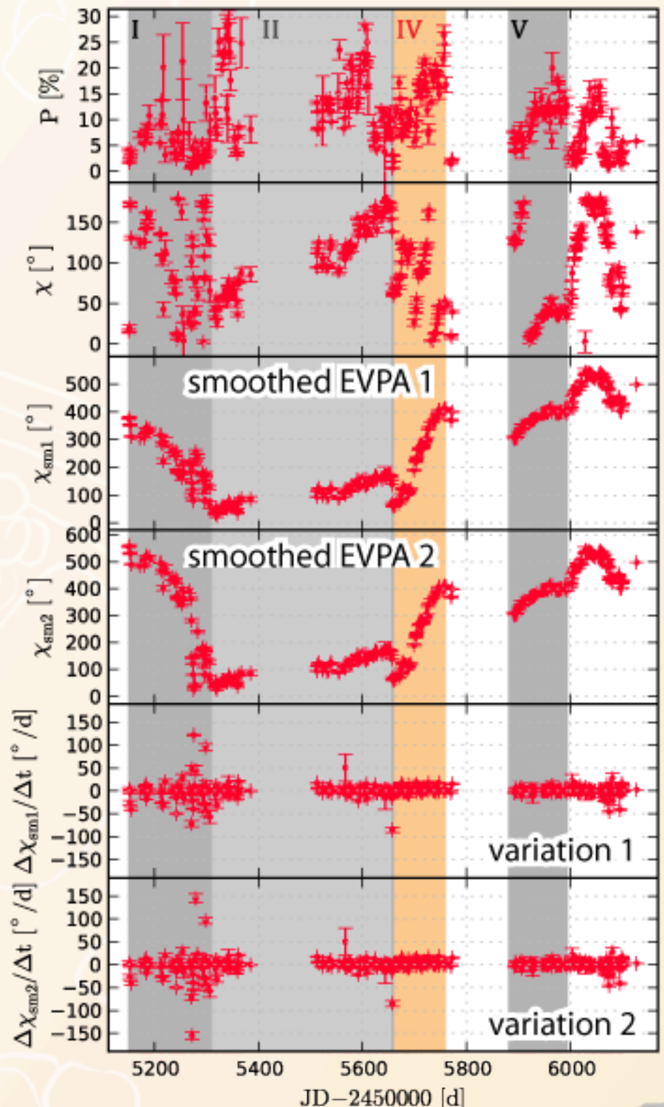

Fig. 6e: 3C 279 optical polarization

IV. Polarization of 3C 279

IV.a EVPA smoothness

Epoch	EVPA	s [°/d]	$\chi_{sm1} = \chi_{sm2}$
I	↓	32(5)	no
II	↑		
III	↓		
IV	↑	2-6	yes
V	↑		
VI	↑		

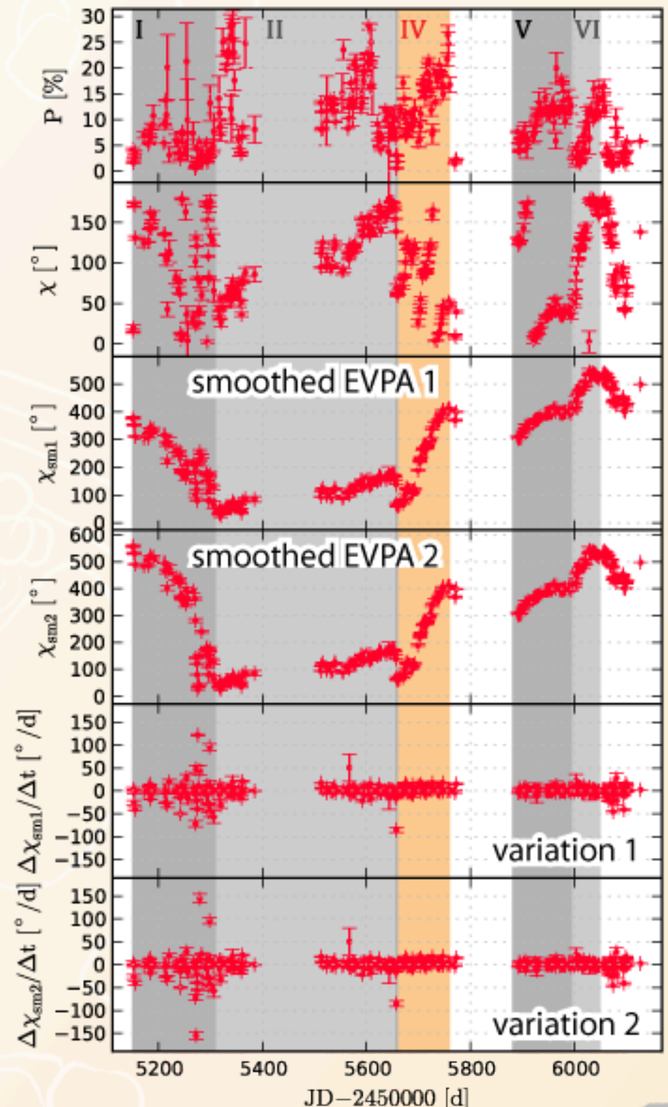

Fig. 6f: 3C 279 optical polarization

Sebastian Kiehlmann, Dipl.-Phys.
Max-Planck Institut für Radioastronomie, Bonn

IV. Polarization of 3C 279

IV.a EVPA smoothness

Epoch	EVPA	s [°/d]	$\chi_{sm1} = \chi_{sm2}$
I	↓	32(5)	no
II	↑		
III	↓		
IV	↑	2-6	yes
V	↑		
VI	↑		
VII	↓	10.5(8)	yes

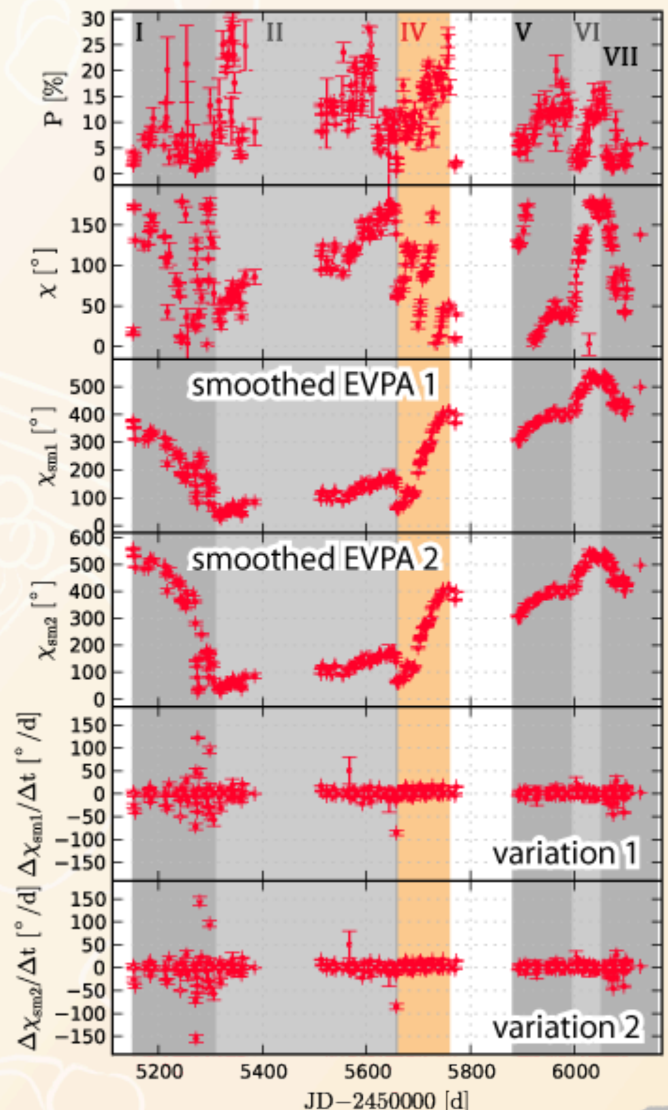

Fig. 6g: 3C 279 optical polarization

Sebastian Kiehlmann, Dipl.-Phys.
Max-Planck Institut für Radioastronomie, Bonn

IV. Polarization of 3C 279

IV.b Interpretation

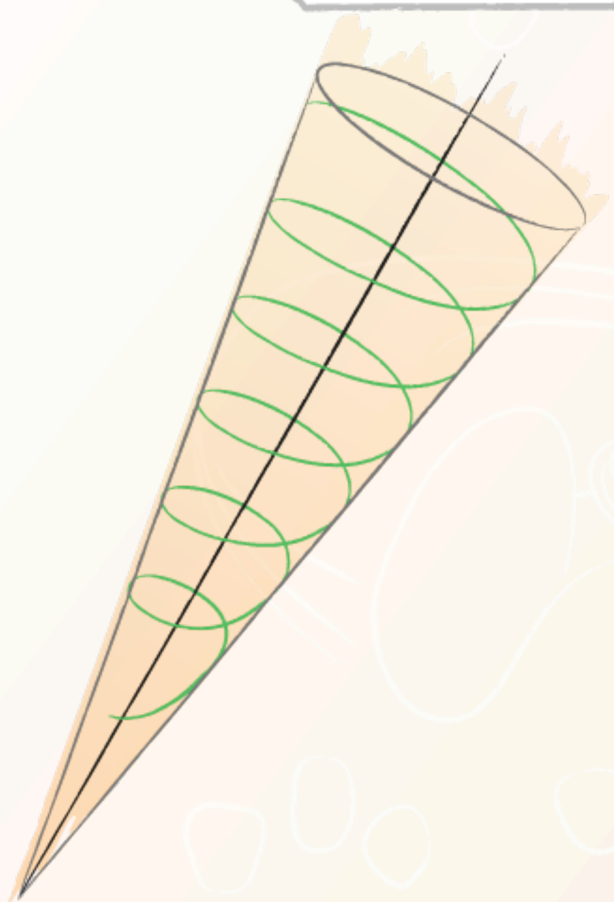

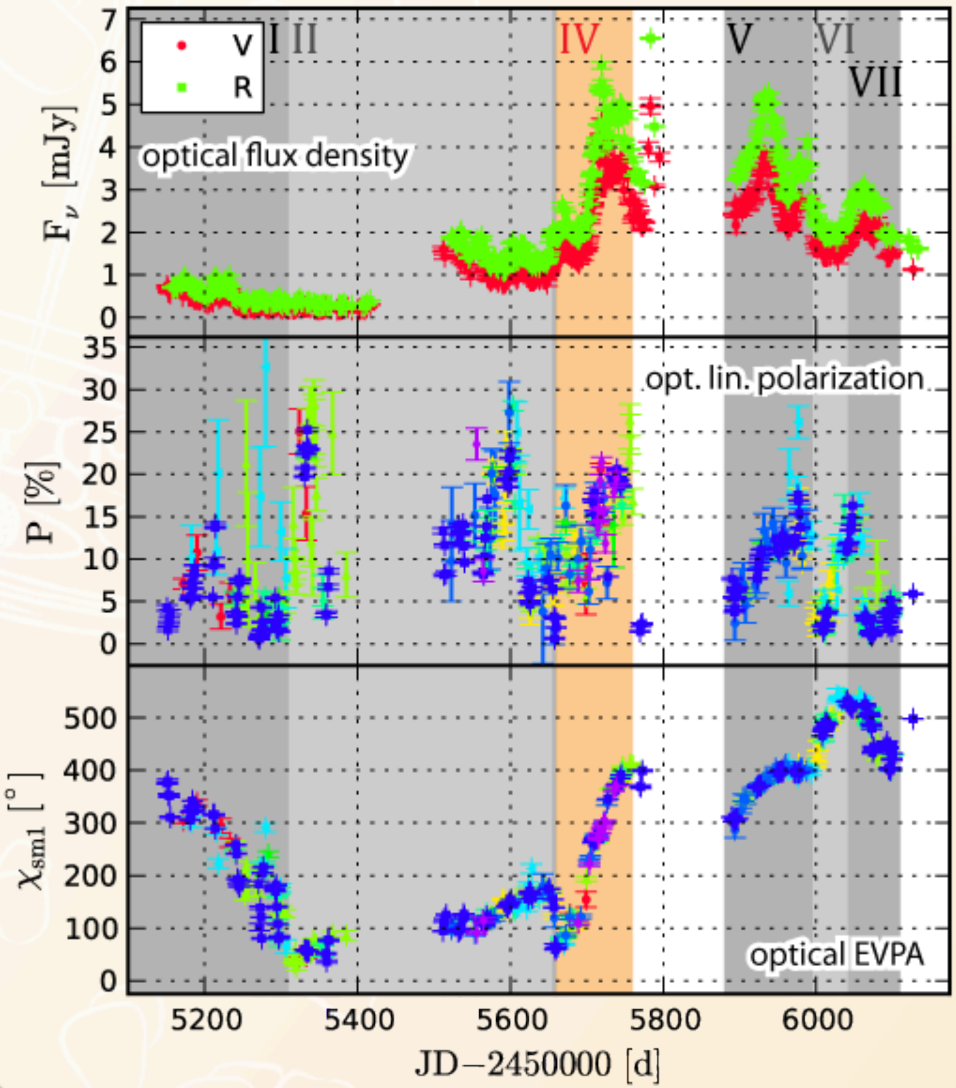

Fig. 7a: Sketched jet model

Fig. 8: 3C 279 LCs (V+R) and opt. pol.

Sebastian Kiehlmann, Dipl.-Phys.
Max-Planck Institut für Radioastronomie, Bonn

IV. Polarization of 3C 279

IV.b Interpretation

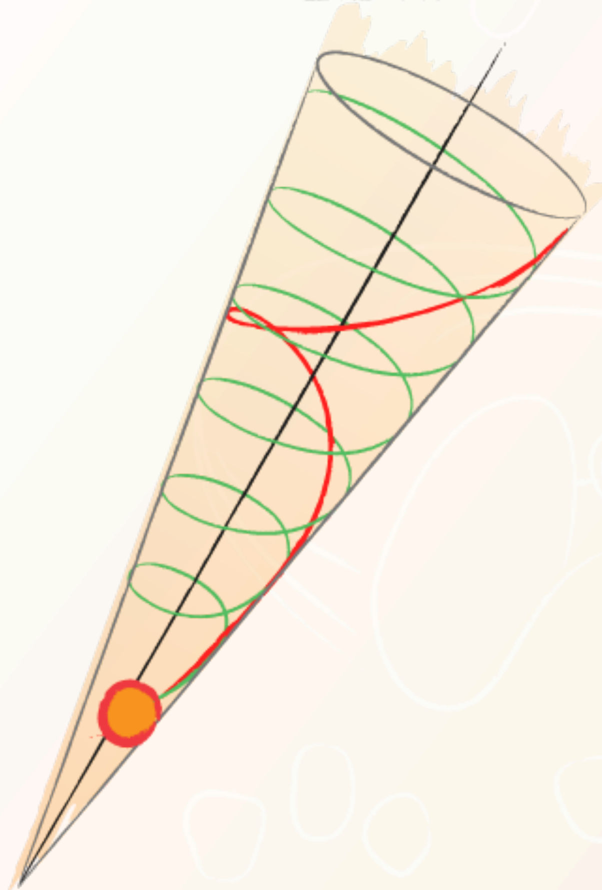

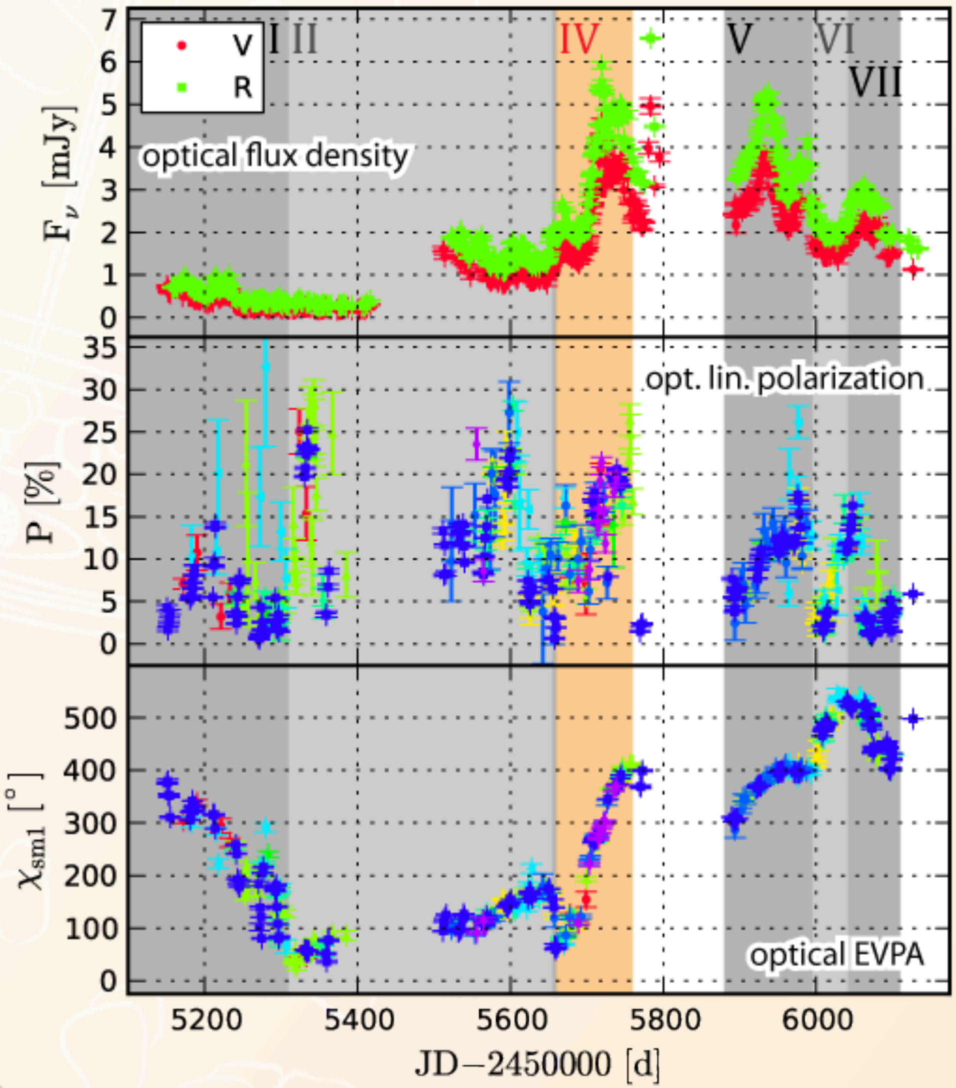

Fig. 7b: Sketched jet model

Fig. 8: 3C 279 LCs (V+R) and opt. pol.

Sebastian Kiehlmann, Dipl.-Phys.
Max-Planck Institut für Radioastronomie, Bonn

IV. Polarization of 3C 279

IV.c Gamma-ray-flaring

Event time:

$\Delta t \approx 110\ d$

Assuming Lorentz factor:

$\Gamma = 15$

Traveling distance:

$\Delta r \sim 5 \cdot 10^5\ r_S$

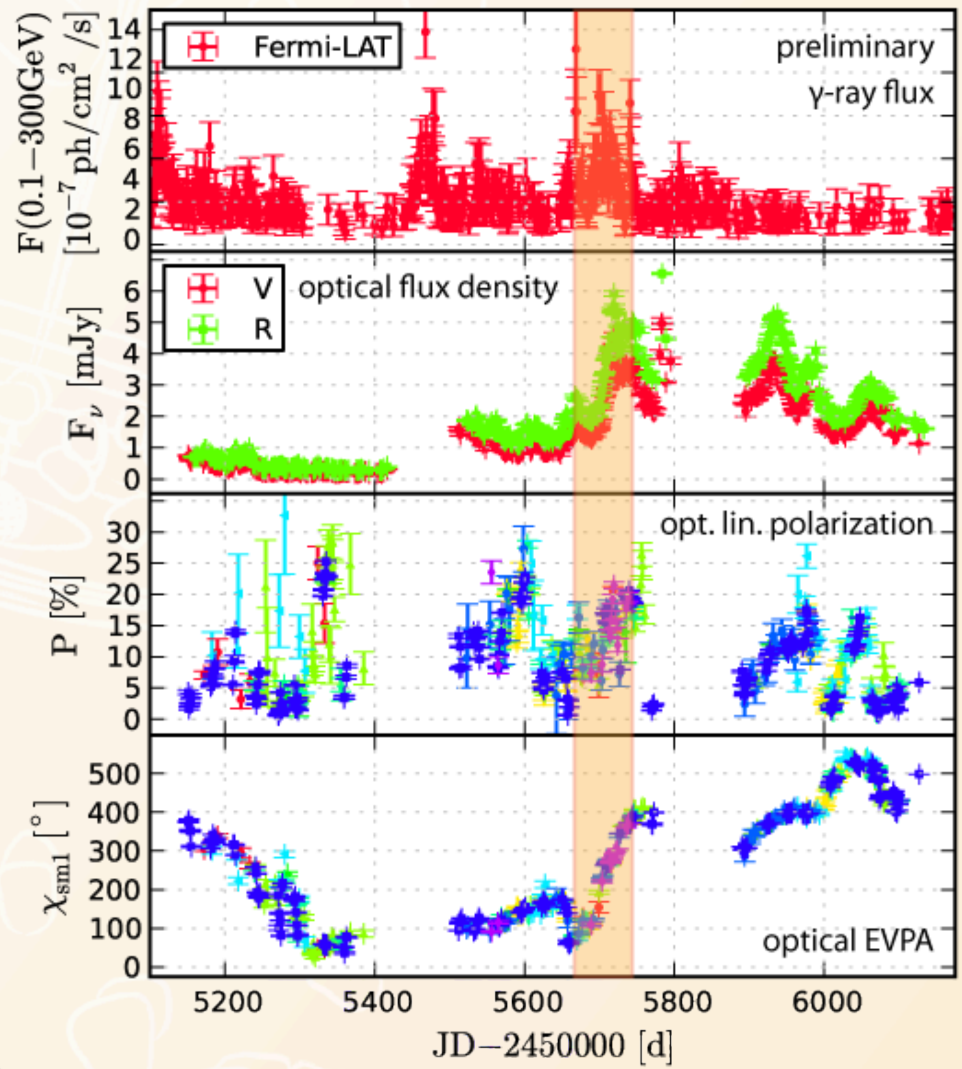

Fig. 9: 3C 279 γ-ray light curve, optical light curves and polarization

IV. Polarization of 3C 279

IV.d mm polarization

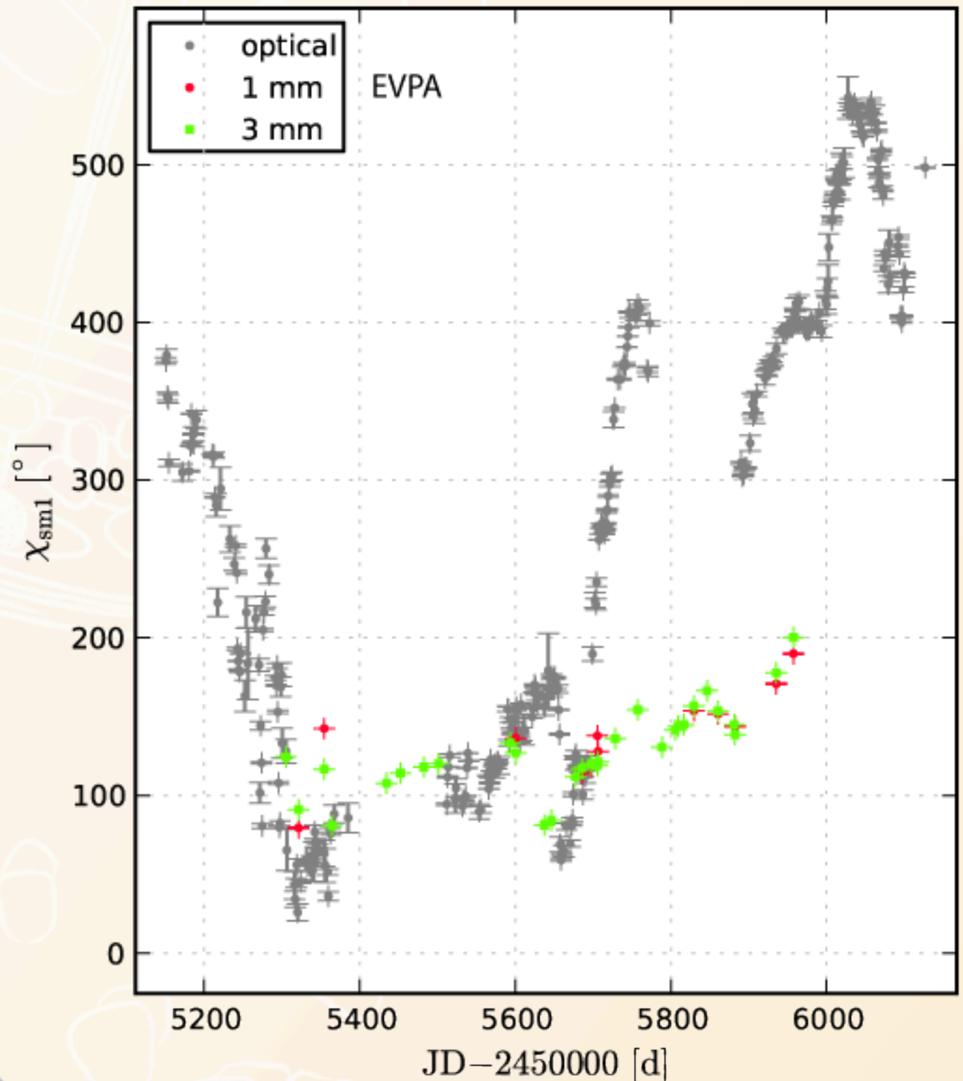

Fig. 10: 3C 279 mm and optical EVPA

v. Conclusions

Method:

- Distinguish stochastic from deterministic EVPA variation.

3C 279 :

- Possibly stochastic EVPA variation during low-state
- Deterministic EVPA variation during flaring state
  - EVPA rotation $>360°$ → no globally bending jet
    → helical motion in a helical magnetic field
  - Two-directional

Special thanks to the QMP collaborators:

T. Savolainen (PI), S.G. Jorstad, F. Schinzel, K.V. Sokolovsky, I. Agudo, M. Aller, L. Berdnikov, V. Chavushyan, L. Fuhrmann, M. Gurwell, R. Itoh, J. Heidt, Y.Y. Kovalev, T. Krajci, O. Kurtanidze, A. Lähteenmäki, V.M. Larionov , J. León-Tavares, A.P. Marscher, K. Nilson, the AAVSO, the Yale SMARTS project and all the observers.

The Quasar Movie Project

Acknowledgements:

SK was supported for this research through a stipend from the International Max Planck Research School (IMPRS) for Astronomy and Astrophysics at the Max Planck Institute for Radio Astronomy in cooperation with the Universities of Bonn and Cologne.

Data from the Steward Observatory spectropolarimetric monitoring project were used. This program is supported by Fermi Guest Investigator grants NNX08AW56G, NNX09AU10G, and NNX12AO93G.

We acknowledge with thanks the variable star observations from the AAVSO International Database contributed by observers worldwide and used in this research.

MAX-PLANCK-GESELLSCHAFT

IMPRS astronomy & astrophysics Bonn and Cologne